

Zero Energy Bound States on Nano Atomic Line Defect in Iron-based High Temperature Superconductors

Degang Zhang^{1,2,3}

¹College of Physics and Electronic Engineering, Sichuan Normal University, Chengdu 610101, China

²Institute of Solid State Physics, Sichuan Normal University, Chengdu 610101, China

³Texas Center for Superconductivity and Department of Physics, University of Houston, Houston, Texas 77204, USA

Motivated by recent scanning tunneling microscopy experiments on Fe atomic line defect in iron-based high temperature superconductors, we explore the origin of the zero energy bound states near the endpoints of the line defect by employing the two-orbit four-band tight binding model. With increasing the strength of the Rashba spin-orbit coupling along the line defect, the zero energy resonance peaks move simultaneously forward to negative energy for s_{+-} pairing symmetry, but split for s_{++} pairing symmetry. The superconducting order parameter correction due to As(Te, Se) atoms missing does not shift the zero energy resonance peaks. Such the zero energy bound states are induced by the weak magnetic order rather than the strong Rashba spin-orbit coupling on Fe atomic line defect.

PACS numbers: 71.10.Fd, 71.18.+y, 71.20.-b, 74.20.-z

1. INTRODUCTION

Since the discovery of cuprates in 1986 [1], high temperature superconductivity has been a focus of both theoretical and experimental investigations in condensed matter physics. After twenty-two years, another family of high temperature superconductors, i.e. iron-based superconductors, was also found in 2008 [2]. Such the superconductors with high transition temperatures usually possess the layered crystal structures consisting of the conducting planes, e.g. the CuO_2 planes in the cuprates and the Fe-As(Te, Se) layers in the iron-based superconductors. It is known that the ligand O or As(Te, Se) atoms not only affect heavily the energy band structures, but also play a crucial role in forming the superconducting pairing symmetries. The O atoms on the Cu-Cu bonds lead to the d-wave order parameter in the cuprates while the As(Te, Se) atoms above and below the center of each face of the Fe square lattice induce the s_{+-} or s_{++} pairing symmetry due to the predominant spin fluctuations or the orbital fluctuations in the iron-based superconductors. These superconducting pairing symmetries can be identified by a nonmagnetic impurity in the conducting planes, which produces a zero energy [3-9] or in-gap bound states or no resonance peaks in the local density of states (LDOS) [10,11].

In order to understand the mechanics of high temperature superconductivity, we first find out the role of the ligands in the high temperature superconductors. In Ref. [11], a single As vacancy on the surface of optimally electron-doped $\text{BaFe}_{2-x}\text{Co}_x\text{As}_2$ was investigated by performing scanning tunneling microscopy (STM) experiments. A pair of in-gap resonance peaks on the As vacancy was observed. Such the in-gap bound states can be explained successfully by the two-orbit four-band tight binding model, which takes the asymmetric effect of up

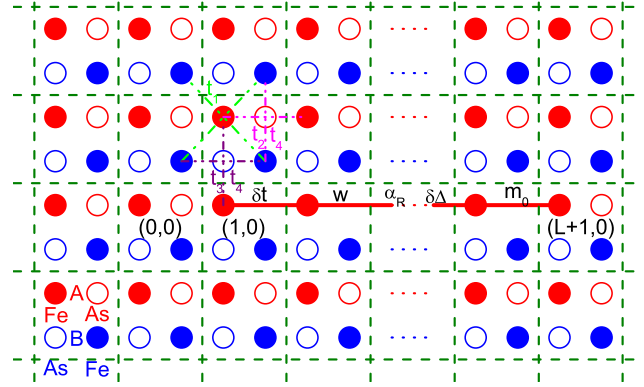


FIG. 1: (Color online) Schematic of the atomic line defect produced by L As (Te, Se) vacancies in the Fe-As (Te, Se) layer with each unit cell containing two Fe (A and B) and two As (Te, Se) (A and B) ions. The As (Te, Se) ions A and B are located just above and below the center of each face of the Fe square lattice, respectively. Here, t_1 is the nearest neighboring hopping between the same orbitals d_{xz} or d_{yz} , t_2 and t_3 are the next nearest neighboring hoppings between the same orbitals mediated by the As (Te, Se) ions B and A, respectively, t_4 is the next nearest neighboring hopping between the different orbitals. δt ($W = -t_4$) and $\delta\Delta$ are the local hopping correction between the same (different) orbitals and the superconducting order parameter correction due to the As (Te, Se) vacancies, respectively. α_R and M_0 are the Rashba spin-orbit coupling and the weak magnetic moment on the atomic line defect.

and down ligand As (Te, Se) atoms on the surface Fe-As (Te, Se) layer into account [10,12]. Recently, a nano Fe atomic line defect (ALD) (see Fig. 1), which is produced by missing a line of Te/Se atoms in one-unit-cell-thick $\text{FeTe}_{0.5}\text{Se}_{0.5}$ films grown on $\text{SrTiO}_3(001)$ substrates, was also studied by using STM [13]. The robust zero energy resonance peaks (ZERPs) in the dI/dV curves show up

near the endpoints of the Fe ALD, which is approximately 6 (3) nm long (short) with 15 (8) Te/Se atoms missing, but disappear at the middle part of the long Fe ALD. The ZERPs are produced due to the strong Rashba spin-orbit coupling (SOC) along the Fe ALD with the inversion symmetry breaking [14]. However, it is hard to induce the strong Rashba SOC along the nano Fe ALD. In addition, the authors in Ref. [13] do not rule out that the Fe ALD becomes magnetic as the missing Te/Se atoms in the top sublayer remove half of the spin-orbit coupled Fe-chalcogen bonds. In this work, we present another explanation of the ZERPs, which are produced by the weak magnetic order on the Fe ALD. Such a mechanism perfectly fits the STM observations [13]. Here we employ the two-orbit four-band tight binding model mentioned above in order to investigate the influence of the nano Fe ALD on the LDOS [10]. The empirical energy band model can exhibit excellently the energy band structure of the iron-based superconductors and its evolution with electron or hole doping measured by ARPES experiments [15-24] and explain successfully a series of STM experiments in iron-based superconductors, e.g. in-gap impurity bound states [10,25], the negative energy resonance peak in the vortex core [26,27], the 90° domain walls and anti-phase domain walls[28-31], the zero-energy bound state induced by the interstitial excess Fe ions[32-34], etc., and especially repeated the phase diagram observed by nuclear magnetic resonance and neutron scattering experiments [35-37]. Very recently, this tight binding model was also used to study the competition among the superconducting order, the magnetic order, and the kinetic energy in europium-based iron pnictides [38].

2. MODEL OF ALD

The Hamiltonian describing the Fe ALD in iron-based superconductors can be written as

$$H = H_0 + H_{\text{BCS}} + H_{\text{ALD}}, \quad (1)$$

where H_0 and H_{BCS} are the two-orbit four-band tight binding model and the mean field BCS pairing Hamiltonian in the Fe-Fe plane, respectively [10], H_{ALD} is the Hamiltonian induced by the As (Te, Se) vacancies on a

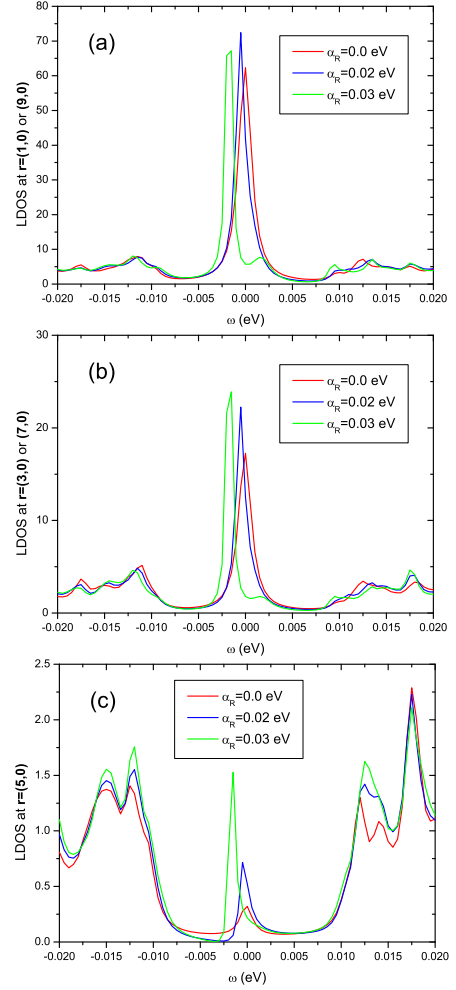


FIG. 2: (Color online) The LDOS on the different Fe sites of the atomic line defect as a function of the bias voltage ω under different α_R at optimal electron doping (15%) for s_{+-} pairing symmetry $\Delta_{uv\mathbf{k}} = \frac{1}{2}\Delta_0(\cos k_x + \cos k_y)$. Here, $\Delta_0 = 0.018$ eV is the large superconducting energy gap measured by STM experiments, $\delta t = 0.4$ eV, $\delta\Delta = 0.0$ eV, and $M_0 = 0.02$ eV.

line, which has general form

$$\begin{aligned}
H_{\text{ALD}} = & \sum_{j=1}^L \{ \delta t \sum_{\alpha\sigma} [c_{A\alpha(j,0)\sigma}^\dagger c_{A\alpha(j+1,0)\sigma} \\
& + c_{B\alpha(j,0)\sigma}^\dagger c_{B\alpha(j,1)\sigma} + \text{h.c.}] \\
& + W \sum_{\alpha\sigma} [c_{A\alpha(j,0)\sigma}^\dagger c_{A1-\alpha(j+1,0)\sigma} \\
& + c_{B\alpha(j,0)\sigma}^\dagger c_{B1-\alpha(j,1)\sigma} + \text{h.c.}] \\
& + \delta\Delta \sum_{\alpha} [c_{A\alpha(j,0)\uparrow}^\dagger c_{A\alpha(j+1,0)\downarrow} \\
& + c_{A\alpha(j,0)\downarrow}^\dagger c_{A\alpha(j+1,0)\uparrow} \\
& + c_{B\alpha(j,0)\uparrow}^\dagger c_{B\alpha(j,1)\downarrow} \\
& + c_{B\alpha(j,0)\downarrow}^\dagger c_{B\alpha(j,1)\uparrow} + \text{h.c.}] \\
& + i\alpha_R \sum_{\alpha\sigma\sigma'} [c_{A\alpha(j,0)\sigma}^\dagger s_z^{\sigma\sigma'} c_{A\alpha(j+1,0)\sigma'} \\
& - c_{A\alpha(j+1,0)\sigma}^\dagger s_z^{\sigma\sigma'} c_{A\alpha(j,0)\sigma'}] \} \\
& + M_0 \sum_{j=1}^{L+1} \sum_{\alpha} [c_{A\alpha(j,0)\uparrow}^\dagger c_{A\alpha(j,0)\uparrow} \\
& - c_{A\alpha(j,0)\downarrow}^\dagger c_{A\alpha(j,0)\downarrow}].
\end{aligned} \quad (2)$$

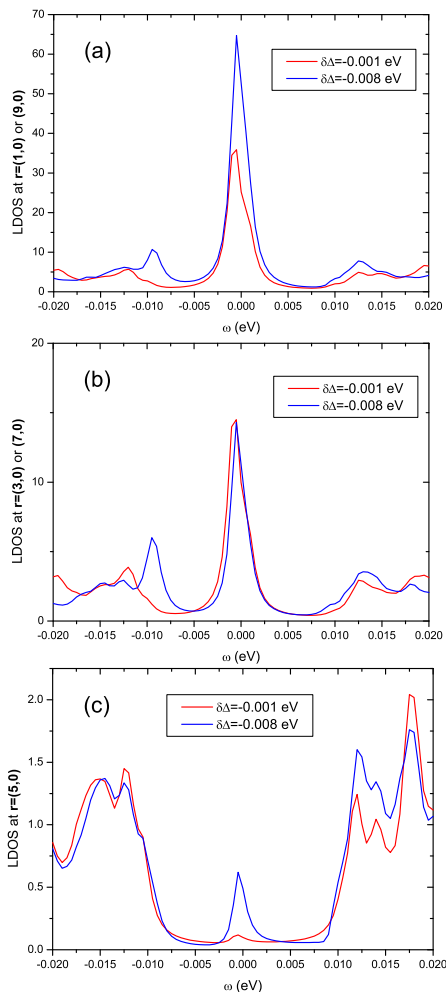


FIG. 3: (Color online) The LDOS on the different Fe sites of the atomic line defect as a function of the bias voltage ω under different $\delta\Delta$ at optimal electron doping (15%) for s_{+-} pairing symmetry $\Delta_{uv\mathbf{k}} = \frac{1}{2}\Delta_0(\cos k_x + \cos k_y)$. Here, $\Delta_0 = 18.0$ meV is the large superconducting energy gap measured by STM experiments, $\delta t = 0.4$ eV, $\alpha_R = 0.008$ eV, and $M_0 = 0.02$ eV.

Here, $\alpha = 0$ and 1 represent the degenerate orbitals d_{xz} and d_{yz} , respectively, s_z is the Pauli matrix along the z direction, $c_{A(B),\alpha,(i,j),\sigma}^\dagger$ ($c_{A(B),\alpha,(i,j),\sigma}$) creates (destroys) an α electron with spin σ ($=\uparrow$ or \downarrow) in the unit cell (i, j) of the Fe sublattice A (B). δt (W) is the local hopping correction between the same (different) orbitals due to the As (Te, Se) vacancies. Because the As (Te, Se) vacancies cannot mix d_{xz} orbital and d_{yz} orbital, we always have $W = -t_4$. $\delta\Delta$ is the superconducting order parameter correction, α_R is the Rashba SOC induced by the inversion symmetry breaking along the Fe ALD, and M_0 is the magnetic moment produced by the asymmetric environments around the Fe ALD.

After introducing first the Fourier transformations $c_{A(B)\alpha(i,j)\sigma} = \frac{1}{\sqrt{N}} \sum_{\mathbf{k}} c_{A(B)\alpha\mathbf{k}\sigma} e^{i(k_x x_i + k_y y_j)}$ with N the number of unit cells and the canonical transformations

for $c_{A,\alpha,\mathbf{k},\sigma}$ and $c_{B,\alpha,\mathbf{k},\sigma}$, and then taking the Bogoliubov transformations for new fermion operators, we can also solve analytically the Hamiltonian H for the Fe ALD in iron-based superconductors by using the T-matrix approach [10,12,33]. The analytic formulas for the Green's functions in momentum space have been derived. The LDOS on the Fe ALD at different bias voltages can be obtained through the Fourier transformation of the Green's functions in momentum space and $i\omega_n \rightarrow \omega + i\delta$. In order to compare with the STM experiments [13], here we have calculated the short Fe ALD ($L=8$) in a square Fe lattice with $N = 60 \times 60$ unit cells, which is enough to ensure the accuracy of theoretical results. In our calculations, we have used the energy band parameters: $t_1 = -0.5$ eV, $t_2 = -0.2$ eV, $t_3 = 1.0$ eV, and $t_4 = -0.02$ eV, which are same with the previous works [10,12,27,30,31,33,34,37,38], the chemical potential $\mu = -0.49$ eV corresponding to 15% electron doping, the hopping correction $\delta t = 0.4$ eV, the superconducting energy gap $\Delta_0 = 18$ meV observed by the STM experiments on the one-unit-cell-thick FeTe_{0.5}Se_{0.5} films grown on SrTiO₃(001) substrates [13], and $\delta = 0.0008$ eV.

3. RESULTS AND DISCUSSION

We plot the curves of the LDOS on the Fe ALD as a function of the bias voltage ω under different α_R at the optimal electron doping (15%) for the s_{+-} pairing symmetry $\Delta_{uv\mathbf{k}} = \frac{1}{2}\Delta_0(\cos k_x + \cos k_y)$ in Figs. 2, where $\Delta_0 = 0.018$ eV, $\delta t = 0.4$ eV, $\delta\Delta = 0.0$ eV, and $M_0 = 0.02$ eV. Obviously, when α_R is weak, the LDOS at the different sites of the Fe ALD have a zero energy resonance peak (ZERP). The height of the ZERP rapidly decays with the distance to the endpoint of the Fe ALD. Such a feature of the ZERP coincides qualitatively with the STM observations [13]. With increasing α_R , the ZERPs move simultaneously forward to the bias voltage. We note that if α_R exceeds a critical value, the LDOS at the midpoint, i.e. $\mathbf{r} = (5, 0)$, is negative under some bias voltages, which is unphysical (see Fig. 2c). Therefore, the Rashba SOC on the Fe ALD is not too strong.

Fig. 3 shows the LDOS on the Fe ALD as a function of the bias voltage ω under different $\delta\Delta$ at the optimal electron doping (15%) for the s_{+-} pairing symmetry when $\alpha_R = 0.008$ eV. With increasing $|\delta\Delta|$, the location of the ZERP keeps unchanged. However, the ZERP becomes higher at the endpoint $\mathbf{r} = (1, 0)$ or $\mathbf{r} = (9, 0)$ and the midpoint $\mathbf{r} = (5, 0)$. Meanwhile, the locations of the superconducting coherence peaks (SCP) have a large shift forward to zero energy near the endpoints of the Fe ALD and seem not to change at the midpoint.

In Fig. 4, we depict the LDOS on the Fe ALD as a function of the bias voltage ω under different α_R at the optimal electron doping (15%) for the s_{++} pairing symmetry $\Delta_{uv\mathbf{k}} = \frac{1}{2}\Delta_0|(\cos k_x + \cos k_y)|$ when $\Delta_0 = 0.018$

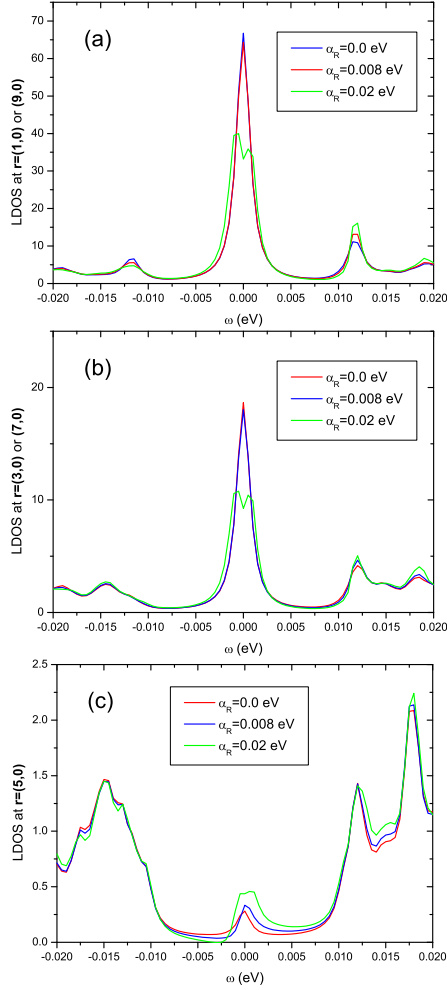


FIG. 4: (Color online) The LDOS on the different Fe sites of the atomic line defect as a function of the bias voltage ω under different α_R at optimal electron doping (15%) for s_{++} pairing symmetry $\Delta_{uv\mathbf{k}} = \frac{1}{2}\Delta_0|\cos k_x + \cos k_y|$. Here, $\Delta_0 = 0.018$ eV is the large superconducting energy gap measured by STM experiments, $\delta t = 0.4$ eV, $\delta\Delta = 0.0$ eV, and $M_0 = 0.025$ eV.

eV, $\delta t = 0.4$ eV, $\delta\Delta = 0.0$ eV, and $M_0 = 0.025$ eV. If α_R is small, the LDOS at the different sites also possess a ZERP. The height of the ZERP also decreases rapidly with the distance to the endpoint of the Fe ALD, similar to the case of the s_{+-} pairing symmetry in Fig. 2. When α_R becomes larger, the ZERPs simultaneously split, but the locations of the SCP are not shifted. Obviously, α_R also has a critical value, at which the LDOS at the midpoint is negative under some bias voltages.

Fig. 5 exhibits the LDOS on the Fe ALD as a function of the bias voltage ω under different $\delta\Delta$ at the optimal electron doping (15%) for the s_{++} pairing symmetry. With increasing $|\delta\Delta|$, the ZERP does not move. The locations of the SCP also have a large shift near the endpoints of the Fe ALD and seem not to change at the midpoint, consistent with the case of the s_{+-} pairing symmetry in Fig. 3.

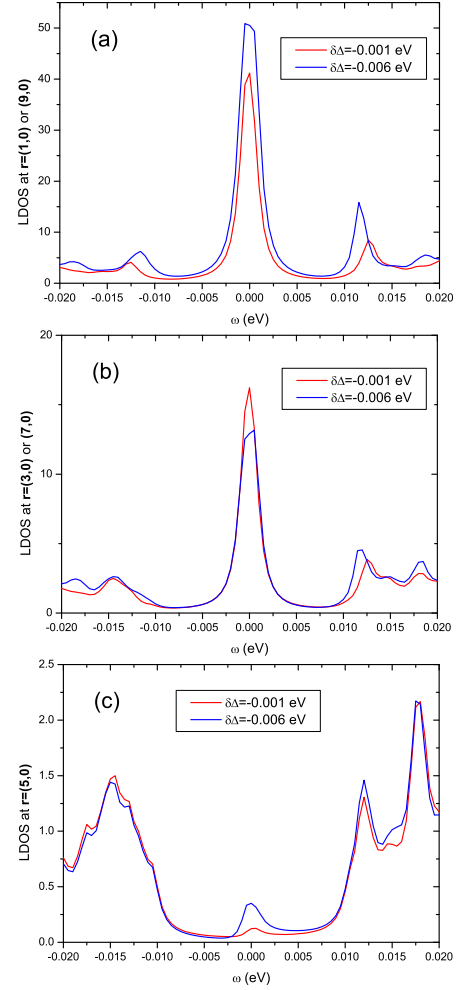


FIG. 5: (Color online) The LDOS on the different Fe sites of the atomic line defect as a function of the bias voltage ω under different $\delta\Delta$ at optimal electron doping (15%) for s_{++} pairing symmetry $\Delta_{uv\mathbf{k}} = \frac{1}{2}\Delta_0|\cos k_x + \cos k_y|$. Here, $\Delta_0 = 18.0$ meV is the large superconducting energy gap measured by STM experiments, $\delta t = 0.4$ eV, $\alpha_R = 0.008$ eV, and $M_0 = 0.025$ eV.

In summary, we have explored the impact of As (Te, Se) atoms missing on the electronic states at the Fe ALD in iron-based superconductors. When the Rashba SOC α_R and the magnetic order M_0 are weak, a ZERP appears apparently near the endpoints of the Fe ALD for both s_{+-} and s_{++} pairing symmetries. The height of the ZERP decays rapidly with increasing the distance to the endpoint. We note that the ZERP vanishes at the middle part of a long Fe ALD. Such the ZERPs are consistent qualitatively with the STM experiments [13]. Here we have presented another origin of the ZERPs, which is due to the weak magnetic order rather than the strong Rashba SOC on the Fe ALD. Such a weak magnetic order could be detected by neutron scattering experiments.

ACKNOWLEDGEMENTS

This work was supported by the Sichuan Normal University, the "Thousand Talents Program" of Sichuan Province, China, the Texas Center for Superconductivity at the University of Houston, and by the Robert A. Welch Foundation under grant No. E-1146.

-
- [1] J. G. Bednorz and K. A. Muller, *Zeitschrift Fur Physik B* **64**,189 (1986).
 [2] Y. Kamihara *et al.*, *J. Am. Chem. Soc.* **130**, 3296 (2008).
 [3] S. H. Pan *et al.*, *Nature* **403**, 746 (2000).
 [4] A. V. Balatsky, I. Vekhter, and J.-X. Zhu, *Rev. Mod. Phys.* **78**, 373 (2006).
 [5] Chia-Ren Hu, *Phys. Rev. Lett.* **72**, 1526 (1994).
 [6] Y. Tanaka and S. Kashiwaya, *Phys. Rev. Lett.* **74**, 3451 (1995).
 [7] M. Sato *et al.*, *Phys. Rev. B* **83**, 224511 (2011).
 [8] M. Covington *et al.*, *Phys. Rev. Lett.* **79**, 277 (1997).
 [9] J. Y. T. Wei *et al.*, *Phys. Rev. Lett.* **81**, 2542 (1998).
 [10] Degang Zhang, *Phys. Rev. Lett.* **103**, 186402 (2009); *ibid.* **104**, 089702 (2010).
 [11] Ang Li *et al.*, *Phys. Rev. B* **99**, 134520 (2019).
 [12] Degang Zhang *et al.*, *New J. Phys.* **20**, 052001 (2018).
 [13] Cheng Chen *et al.*, *Nature Physics* **16**, 536 (2020).
 [14] Yi Zhang *et al.*, *Phys. Rev. X* **11**, 011041 (2021).
 [15] H. Ding *et al.*, *Europhys. Lett.* **83**, 47001 (2008).
 [16] D. H. Lu *et al.*, *Nature (London)* **455**, 81 (2008).
 [17] C. Liu *et al.*, *Phys. Rev. Lett.* **101**, 177005 (2008).
 [18] T. Kondo *et al.*, *Phys. Rev. Lett.* **101**, 147003 (2008).
 [19] D. V. Evtushinsky *et al.*, *Phys. Rev. B* **79**, 054517 (2009).
 [20] K. Nakayama *et al.*, *Europhys. Lett.* **85**, 67002 (2009) .
 [21] V. Zabolotnyy *et al.*, *Nature (London)* **457**, 569 (2009).
 [22] K. Terashima *et al.*, *PNAS* **106**, 7330 (2009) .
 [23] Y. Sekiba *et al.*, *New J. Phys.* **11**, 025020 (2009).
 [24] H. Miao *et al.*, *Phys. Rev. B* **85**, 094506 (2012).
 [25] S. Grothe *et al.*, *Phys. Rev. B* **86**, 174503 (2012).
 [26] L. Shan *et al.*, *Nature Phys.* **7**, 325 (2011).
 [27] Yi Gao *et al.*, *Phys. Rev. Lett.* **106**, 027004 (2011).
 [28] T.-M. Chuang *et al.*, *Science* **327**, 181 (2010).
 [29] Guorong Li *et al.*, *Phys. Rev. B* **86**, 060512(R) (2012).
 [30] Huaixiang Huang *et al.*, *Phys. Rev. B* **83**, 134517 (2011).
 [31] Bo Li *et al.*, *New J. Phys.* **15**, 103018 (2013).
 [32] J.-X. Yin *et al.*, *Nature Physics* **11**, 543 (2015).
 [33] Degang Zhang, *Physica C* **519**, 43 (2015).
 [34] Huaixiang Huang *et al.*, *Phys. Rev. B* **93**, 064519 (2016).
 [35] Y. Laplace *et al.*, *Phys. Rev. B* **80**, 140501 (2009).
 [36] M.-H. Julien *et al.*, *Europhys. Lett.* **87**, 37001 (2009).
 [37] Tao Zhou, Degang Zhang, and C. S. Ting, *Phys. Rev. B* **81**, 052506 (2010).
 [38] Huai-Xiang Huang, Yu-Qian Cao, and Xin Wan, *Phys. Rev. B* **106**, 144503 (2022).